Time multiplexing super resolution using a Barker-based array

Asaf Ilovitsh,[1,*] Eyal Preter,[1] Nadav Levanon,[2] and Zeev Zalevsky[1]

[1] *Faculty of Engineering, Bar-Ilan University, Ramat-Gan 52900, Israel*

[2] *School of Electrical Engineering, Faculty of Engineering, Tel-Aviv University, Tel-Aviv 69978, Israel*

**Corresponding author: ilovitsh@gmail.com*

Received November 5, 2014; accepted November 30, 2014;
posted December 2, 2014 (Doc. ID 226364); published January 7, 2015

We propose the use of a new encoding mask in order to improve the performance of the conventional time multiplexing super resolution method. The resolution improvement is obtained using a 2D Barker-based array that is placed upon the object and shifted laterally. The Barker-based array is a 2D generalization of the standard 1D Barker code. The Barker-based array has stable autocorrelation sidelobes, making it ideal for the encoding process. A sequence of low resolution images are captured at different positions of the array, and are decoded properly using the same array. After removing the low resolution image from the resulting reconstruction, a high resolution image is established. The proposed method is presented analytically, demonstrated via numerical simulation, and validated by laboratory experiment.

OCIS codes: (100.6640) Superresolution; (100.0100) Image processing.
http://dx.doi.org/10.1364/OL.40.000163

The resolution of an imaging lens with a finite aperture is limited by diffraction. The minimum distance between two nearby points that still allows for separation between them was pronounced by Abbe to be proportional to the optical wavelength and to the F number of the imaging system [1]. Super resolution (SR) techniques aim to overcome the diffraction limitation. The main concept in SR approaches is that high resolution (HR) spatial information can be obtained if some *a priori* information on the object exists. Using this *a priori* information one may sacrifice other dimensions in order to achieve information in the spatial domain [2–5]. The sacrificed axes, which may be used for multiplexing the additional spatial resolution, can be, for instance, time [6,7], wavelength [8,9], field of view [10,11], polarization [12,13], dynamic range [14,15], etc.

Time multiplexing super resolution (TMSR) is perhaps the most common SR technique that overcomes the diffraction limitation. The original concept, suggested by Francon [6], included two scanning pinholes, one at the object plane, and one in the image plane. This method is highly time consuming, since the entire object needs to be scanned point by point. A second approach was suggested by Lukosz [7], and included two moving gratings. The first grating is placed near the object and is used for encoding the spatial information. The second grating is placed near the detector, or added digitally by computer means [16], and is used for decoding the spatial information. The two gratings are shifted between frames during the imaging sequence. For a 1D SR, the grating shift is relatively simple. However, in order to achieve 2D SR, the gratings need to be shifted in both directions. Another approach is using a random noise as the encoding and decoding masks [17]. This method relies on the autocorrelation (AC) of the random noise mask. Since the noise is random in all directions, a 1D shift can achieve 2D SR. However, the variance of the sidelobes of the AC is on the order of the square root of the number of images. Thus, reducing the variance of the sidelobes requires a great number of images, usually hundreds. Another method is regarding the SR process as an inverse problem [18]. This method has an inherent difficulty, which is to avoid amplifying the noise during the inverse process (this is common for all inverse problems). In addition, the system matrix itself is ill conditioned, presenting the challenge of inverting the matrix in a numerically stable fashion [19].

In this Letter we propose using a binary transmission Barker-based array as the encoding and decoding mask in the conventional TMSR method. The proposed array is a 2D generalization of the 1D Barker code [20], which is widely used in radar signals [21]. The proposed method has several advantages over the previous ones; a 1D scanning generates 2D SR, regardless of the scanning direction. The process requires significantly less images than the random noise method. The method does not require an inverse process, and thus noises effects will not be amplified during the SR process.

A Barker code is a bipolar sequence at length N, where each bit has a value of −1 or 1. This sequence has an ideal aperiodic AC property such that the peak magnitude equals N and the sidelobe magnitudes are 0 or 1. All the Barker codes exhibit a two-valued cyclic (periodic) AC, namely constant sidelobes values. In optical amplitude masks −1 is not a legitimate value and thus each −1 in the Barker code is replaced by 0. The modified (unipolar) Barker sequence maintains the property of a two-valued cyclic AC.

A 2D unipolar Barker array will be optimal for TMSR. Unfortunately, this kind of array does not exist for more than a 2×2 array [22,23]. Instead, a generalization of the Barker code into a 2D array was performed as follows: the first row in the array is a standard 1D Barker code, and each row in the array is shifted with respect to the previous row.

The longest reported Barker code is 13 bits long [24]. Using its unipolar representation [1111100110101], a 13×13 array was established. The process is as follows. Each row in the array is shifted 5 pixels to the right in respect to the previous row. This 2D array is presented in Fig. 1(a). One may notice that by using the 5 pixels shift between rows, each column in the array is a cyclic

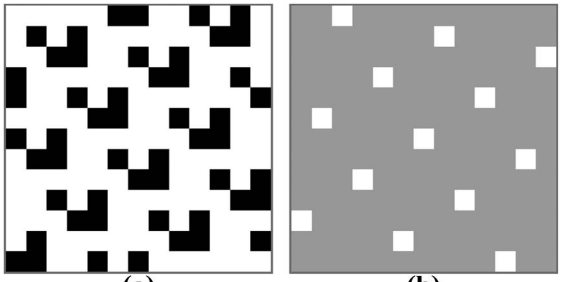

Fig. 1. (a) 13 × 13 Barker-based array, where each row is a 5 pixel shift of the previous row; (b) cyclic AC of the 13 × 13 Barker-based array. Pixel values: white, 1, gray, 2/3, black, 0.

shift of a 13-bit Ipatov code [1110010111110] [21] which, while not Barker, also exhibits a two-valued cyclic AC. The cyclic AC of the 13 × 13 example is presented in Fig. 1(b). The cyclic AC has N peaks equal to 1, with a distance between each two peaks of $\sqrt{13}$. The sidelobes between the peaks have a constant value of 2/3.

Following the conventional TMSR 4f system (presented in Fig. 2), the blurred output intensity before the second mask is given by

$$I_{\text{img}}(x,y,t) = \int_{-\infty}^{\infty}\int_{-\infty}^{\infty} I_{\text{obj}}(x',y') M_1(x'-vt,y')p(x-x',y-y')\mathrm{d}x'\mathrm{d}y', \tag{1}$$

where I_{obj} is the object intensity, M_1 is the encoding mask, v is its velocity, and p is the point spread function (PSF).

The decoding process involves multiplying each image with the appropriate decoding mask, M_2, and integrating over time,

$$R(x,y) = \int_{-\infty}^{\infty} I_{\text{img}}(x,y,t)M_2(x-vt,y)\mathrm{d}t. \tag{2}$$

Since only the masks are time dependent, changing the integral order is allowed. Assuming M_1 and M_2 are the same Barker-based array, denoted by M, the time integral becomes

$$\int_{-\infty}^{\infty} M(x-vt,y)M(x'-vt,y')\mathrm{d}t = \sum \delta(x-x',y-y') + c. \tag{3}$$

The result is a set of Dirac deltas plus a constant [as presented in the 13-bit example in Fig. 1(b)]. Introducing the time integral into Eq. (2) yields

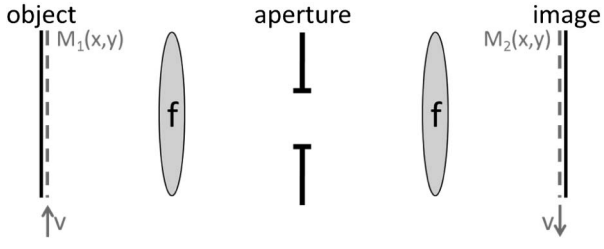

Fig. 2. Conventional TMSR 4f system.

$$R(x,y) = \int_{-\infty}^{\infty}\int_{-\infty}^{\infty} I_{\text{obj}}(x',y')p(x-x',y-y') \left[\sum \delta(x-x',y-y') + c\right]\mathrm{d}x'\mathrm{d}y'. \tag{4}$$

Assuming the PSF is smaller than the distance between two peaks, the integral becomes

$$R(x,y) = p(0,0)I_{\text{obj}}(x,y) + c\cdot \text{LRI}, \tag{5}$$

where LRI is the LR image.

In order to achieve the HR image, the LR image (which is known) needs to be subtracted from the reconstruction. As mentioned before, the method will work as long as the PSF is smaller than the distance between peaks, which in our examples is $\sqrt{13}$ or 3.6 pixels in the image plane.

In the numerical simulation the proposed 13 × 13 array was tested. The Barkar-based masks were cyclic, in order to cover the entire object. The mask speed was 1 pixel per frame. Thirteen LR images that simulated the mask movement were generated. The LR images had a resolution 3 times smaller than the HR images. The suggested process was tested on two different objects: a 1951 USAF target, and a "Lena" image. The SR results for the USAF target are presented in Fig. 3. Figure 3(a) is the HR image, Fig. 3(b) is the LR image, Fig. 3(c) is the reconstructed image using 13 LR images of a moving random mask, and Fig. 3(d) is the SR image using the Barker-based mask. It is clearly seen that the proposed method yields better results than the random mask method.

The "Lena" image was also tested, in order to demonstrate the applicability of the proposed method for a gray scale object. The results for the "Lena" image are presented in Fig. 4. Figure 4(a) is the HR image, Fig. 4(b) is the LR image, and Fig. 4(c) is the SR image.

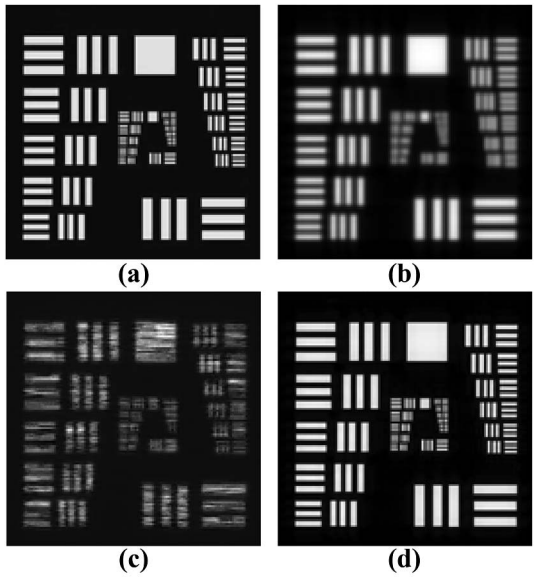

Fig. 3. SR simulation results of a USAF target using the proposed 13 × 13 Barker-based array: (a) HR image, (b) LR image, (c) reconstructed image using a moving random mask, and (d) SR using the Barker-based mask.

Fig. 4. SR simulation results of the "Lena" image using the proposed 13 × 13 Barker-based array: (a) HR image, (b) LR image, and (c) SR image.

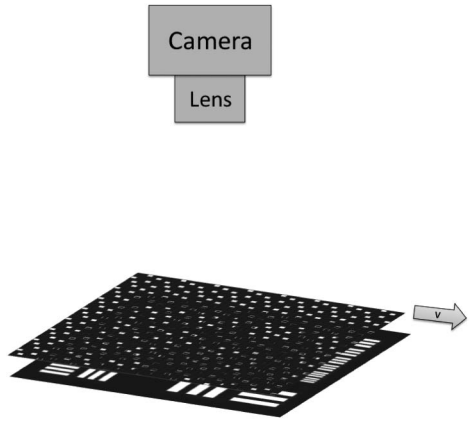

Fig. 5. Experimental setup illustration: a camera looking down on a 1951 USAF target, covered by a moving cyclic Barker-based array.

In order to experimentally test the proposed method, a simple imaging system was built in the laboratory. The object was a USAF target. The mask was a 13 × 13 cyclic Barker-based array with a 1 mm feature size. The mask was placed on top of the object and shifted laterally in 1 mm increments using a linear translation stage. Thirteen LR images were captured using a standard USB camera (Thorlabs DCC1545M) and an 8 mm lens (Navitar NMV-8) located 500 mm above the object. The mask feature size was chosen in order to fulfill the spatial sampling condition [25], making sure that it is sampled at least twice by the camera pixels. This has two implications: first, the resolution improvement is limited to the mask feature size (which is about 3×3 pixels in the object plane), and second, the LR PSF needs to be smaller than the distance between the AC peaks, which in this case is $3 \times \sqrt{13}$ or 10.8 pixels in the image plane. The LR images in the experiment had resolutions about 9 times smaller than HR reference images. The setup illustration is presented in Fig. 5.

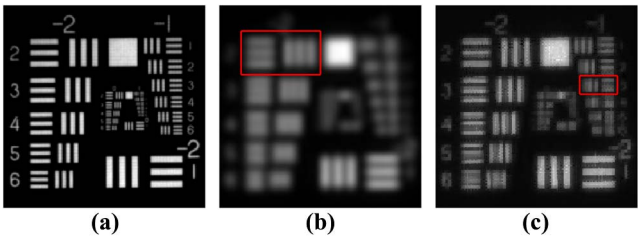

Fig. 6. SR experimental results: (a) HR reference image, (b) LR image, and (c) SR image using the proposed method. The squares represent the last separable frequency in the LR and SR images.

The SR results, obtained using the proposed technique, are presented in Fig. 6. Figure 6(a) is the HR reference image, Fig. 6(b) is the LR image, and Fig. 6(c) is the SR image. The resolution improvement is clearly visible, not only in the marked bars that mark the last separable frequency, but also in the numbers in the target. One may notice that the SR image is pixelated, with a feature size of about 3×3 pixels, due to the feature size of the encoding mask.

To conclude, a new encoding mask for the conventional TMSR method was presented. The mask is a 2D Barker-based array, which is a generalization of the well-known 1D Barker code. Due to the unique AC properties of the proposed array, only a small number of images are required in order to achieve a SR image. The proposed technique was numerically simulated, and laboratory experimented, demonstrating resolution improvement by a factor of 3. Using a fast motorized linear stage for the mask shift, and proper imaging software, the SR process may take less than 1 second.

References

1. R. Otto and L. Fritz, *Die lehre von der bildentstehung im mikroskop von Ernst Abbe* (Vieweg Braunschweig, 1910).
2. I. J. Cox and C. J. R. Sheppard, J. Opt. Soc. Am. A **3**, 1152 (1986).
3. D. Mendlovic and A. W. Lohmann, J. Opt. Soc. Am. A **14**, 558 (1997).
4. G. Toraldo di Francia, J. Opt. Soc. Am. **59**, 799 (1969).
5. Z. Zalevsky, D. Mendlovic, and A. W. Lohmann, Prog. Opt. **XL**, 271 (1999).
6. M. Françon, Nouvo Cimento Suppl. **9**, 283 (1952).
7. W. Lukosz, J. Opt. Soc. Am. **56**, 1463 (1966).
8. A. I. Kartashev, Opt. Spektrosk. **9**, 204 (1960).
9. J. García, V. Micó, D. Cojoc, and Z. Zalevsky, Appl. Opt. **47**, 308 (2008).
10. W. Lukosz and A. Bachl, J. Opt. Soc. Am. **57**, 163 (1966).
11. A. W. Lohmann and M. A. Grimm, J. Opt. Soc. Am. **56**, 1151 (1966).
12. W. Gartner and A. W. Lohmann, Z. Phys. **174**, 18 (1963).
13. A. Whiting, A. Abouraddy, B. Saleh, M. Teich, and J. Fourkas, Opt. Express **11**, 1714 (2003).
14. Z. Zalevsky, P. García-Martínez, and J. García, Opt. Express **14**, 5178 (2006).
15. D. Sylman, V. Micó, J. García, and Z. Zalevsky, Appl. Opt. **49**, 4874 (2010).
16. A. Shemer, D. Mendlovic, Z. Zalevsky, J. Garcia, and P. G. Martinez, Appl. Opt. **38**, 7245 (1999).
17. J. García, Z. Zalevsky, and D. Fixler, Opt. Express **13**, 6073 (2005).
18. S. Farsiu, D. Robinson, M. Elad, and P. Milanfar, Int. J. Imaging Syst. Technol. **14**, 47 (2004).
19. G. H. Golub and C. F. Van Loan, *Matrix Computations* (Johns Hopkins University, 1996).
20. R. H. Barker, *Communication Theory* (Butterworth, 1953), p. 273.
21. N. Levanon and E. Mozeson, *Radar Signals* (Wiley, 2004).
22. S. Alquaddoomi and R. a. Scholtz, IEEE Trans. Inf. Theory **35**, 1048 (1989).
23. J. A. Davis, J. Jedwab, and K. W. Smith, Proc. Am. Math. Soc. **135**, 2011 (2007).
24. R. Turyn and J. Storer, Proc. Am. Math. Soc. **12**, 394 (1961).
25. J. W. Goodman, *Introduction to Fourier Optics* (Roberts & Company, 2005).